Radiative properties of MoS_2 layered crystals

Leonid Kulyuk
Institute of Applied Physics, Academy of Science of Moldova, Chisinau, MD-2028, Republic of Moldova

Luc Charron and Emery Fortin
Department of Physics, University of Ottawa, Ottawa, Ontario K1N 6N5, Canada

(Received 3 April 2003; revised manuscript received 6 June 2003; published 22 August 2003)

Photoluminescence was observed in both synthetic and natural forms of the transition metal dichalcogenide MoS_2. The emission is in the near infrared between 0.8 and 1.2 eV. Two distinct regions were identified. The first region, centered at 1.18 eV and observed only in the synthetic material, is produced by bound excitons related to the halogen transport agent intercalated within the layers during the growth process. The second weaker region, consisting of a broad band centered at 0.95 eV believed to be caused by a deep donor center, was observed in both synthetic and natural molybdenite.

DOI: 10.1103/PhysRevB.68.075314 PACS number(s): 78.55.Hx, 71.35.Gg, 78.67.Pt

I. INTRODUCTION

Molybdenum disulfide (molybdenite) belongs to the family of layered transition metal dichalcogenides (TX_2) characterized by quasi-two-dimensional crystallographic structure.[1,2] Because of a good matching between the solar spectrum and the optical band gaps of the molybdenum and tungsten dichalcogenides and because of a high stability against photocorrosion, these materials are of great interest for application in electrochemical and solid state solar cells.[3,4] In addition 2H-MoS_2 and 2H-WS_2 were the first compounds synthesized as inorganic fullerenlike materials.[5,6] It was shown that fullerenlike molybdenum and tungsten disulfides preserve the semiconducting properties of the layered crystals.[7]

2H-MoS_2 crystallizes in the hexagonal structure (space group $P6_3/mmc$-D^4_{6h}) consisting of covalently bonded S-Mo-S layers linked by weak van der Waals forces. The unit cell contains two layers; the sulfur atoms in one layer are directly above the molybdenum atom in the next. All TX_2 compounds are indirect band gap semiconductors.[4,8,9] This may explain why, in spite of the large number of publications on optical studies, no radiative properties have been reported for the transition metal dichalcogenides before our recent report on 2H-WS_2 and 2H-WSe_2.[10] It was shown that the strong photoluminescence observed in those two synthetic materials is caused by recombination of excitons bound to the neutral centers formed by the intercalation of halogen molecules Br_2 and I_2 in well-defined sites of the van der Waals gap.

This paper presents the first study of the radiative properties of 2H-MoS_2 layered crystals. Synthetic and natural samples were studied. It is shown that the sharp line spectra due to the bound exciton luminescence are characteristic only of the synthetic crystals, while the observed broad-band emission caused by the radiative recombination via a deep level is inherent for both types of samples.

II. EXPERIMENT

The synthetic *n*-type 2H-MoS_2 single crystals were grown by means of chemical vapor transport method, using chlorine Cl_2 as a transport agent. Naturally grown samples were cut from large natural bulk *n*-type molybdenite crystals and then cleaved to produce fresh clean surfaces. The steady-state photoluminescence (PL) measurements were performed with a variable-temperature optical cryostat, a one-meter grating monochromator coupled to a cooled Ge detector, and standard lock-in detection techniques. The luminescence excitation was provided by an Ar-ion laser ($\lambda = 514$ nm) or a diode-pumped cw solid-state laser ($\lambda = 532$ nm). All spectra were corrected for the wavelength-dependent response of the optical system.

A. Characteristic spectra

Figure 1 illustrates PL spectra at 2 and 80 K of a 2H-MoS_2 synthetic crystal. For those crystals, all spectra consist of two characteristic parts: a short-wavelength region with several intense, sharp lines located at about 0.1 eV below the energy of the MoS_2 indirect band gap $E_g^{\mathrm{ind}} = 1.29$ eV (Refs. 8,11) and a broad spectral band (half-width

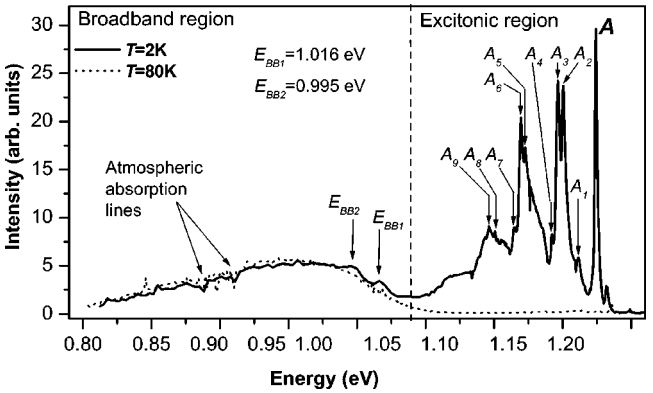

FIG. 1. PL spectra of synthetic 2H-MoS_2 at $T = 2$ and 80 K. Two distinct regions are present: a broadband region and an excitonic region. The broad spectral band contains one- and two-phonon replicas at $T = 2$ K (E_{BB1} and E_{BB2}). At 2 K, the excitonic region contains a zero-phonon line at 1.174 eV (*A*) and phonon replicas (for phonon energies see Table I). At 80 K the excitonic luminescence has almost totally vanished.

TABLE I. Energies of phonon replicas of the *A* line in the photoluminescence spectrum at $T=2$ K (Fig. 1). The energy of the $A_{1g}(\Gamma)$-full symmetric phonon mode of MoS_2 is 50.7 meV (Refs. 13,14).

Notation [a]	Photon energy, eV	Energy shift, meV	Interpretation
A	1.174		Zero-phonon line
A_1	1.162	12.4	Local mode
A_2	1.150	23.7	Local mode
A_3	1.146	27.7	Local mode
A_4	1.142	31.9	Local mode
A_5	1.123	51.6	A_2+A_3
A_6	1.120	54.6	$2A_3$
A_7	1.115	59.1	A_3+A_4
A_8	1.101	73.5	A_2+A_{1g}
A_9	1.096	77.9	A_3+A_{1g}

[a]In order to obtain similar values for the *B* and *C* lines, E_B-$E_A \approx 0.002$ eV and E_C-$E_A \approx 0.012$ eV must be added, respectively, to the energies.

$\Delta_{bb} \approx 0.1$–0.12 eV) centered at $E_{bb}=0.95$ eV. The excitonic region, very prominent in the 2 K spectrum, is usually composed of zero-phonon lines (in this case, a single zero-phonon line is present $E_A=1.174$ eV) followed by phonon replicas (see Table I). The analysis of the phonon replica sideband lines leads to the following four values of phonon energy modes: $E_{\mathrm{ph1}}=12.4$ meV, $E_{\mathrm{ph2}}=23.7$ meV, $E_{\mathrm{ph3}}=27.7$ meV, and $E_{\mathrm{ph4}}=31.9$ meV. These energies differ from those reported for TO and LO phonons in MoS_2 ($E_{\mathrm{TO}} \cong E_{\mathrm{LO}}=48$ meV),[12] as well as from other phonon active modes measured by IR and Raman spectroscopy[13,14] and can be interpreted as local modes induced by the center which provides exciton related luminescence.

As for the broad-band region, its intensity and spectral shape remain largely similar at 2 and 80 K. Phonon replicas of the broad band at $E_{\mathrm{BB1}}=1.017$ eV and $E_{\mathrm{BB2}}=0.996$ eV are observed which will be discussed below. The PL spectra of the natural MoS_2 samples do not reveal any excitonic region. Throughout the whole temperature range only the IR broad-band emission with the same spectral shape- and temperature-dependent behavior as that of the synthetic crystals was detected.

B. Temperature evolution

Figure 2 presents the temperature evolution of the excitonic PL. There are at least three zero-phonon spectral lines contributing to the excitonic emission intensity. The first line, *A* ($E_A=1.174$ eV), can be clearly seen at the lowest temperature only; already at $T=6$ K the *A* line seems to have completely disappeared. However, upon a more detailed observation, the *A* line can be perceived as a shoulder of the second zero-phonon line *B* ($E_B=1{,}176$ eV). Finally, at higher temperatures, the last zero-phonon line *C* ($E_C=1.186$ eV), appears and becomes dominant at $T>60$ K. Increasing the temperature leads to the redistribution of the PL intensity starting from line *A* to line *B*, then from *B* to *C*. At $T>50$ K a fast thermal quenching of the excitonic emission occurs. The broadband luminescence, not shown in Fig. 2, is constant between 2 and 100 K at which point a fast decrease in intensity is initiated. The experimental temperature dependencies of the integral intensity of the excitonic emission $I_{\mathrm{ex}}(T)$ (including the phonon side bands), as well as of the broad band intensity $I_{\mathrm{BB}}(T)$ are presented in Fig. 3.

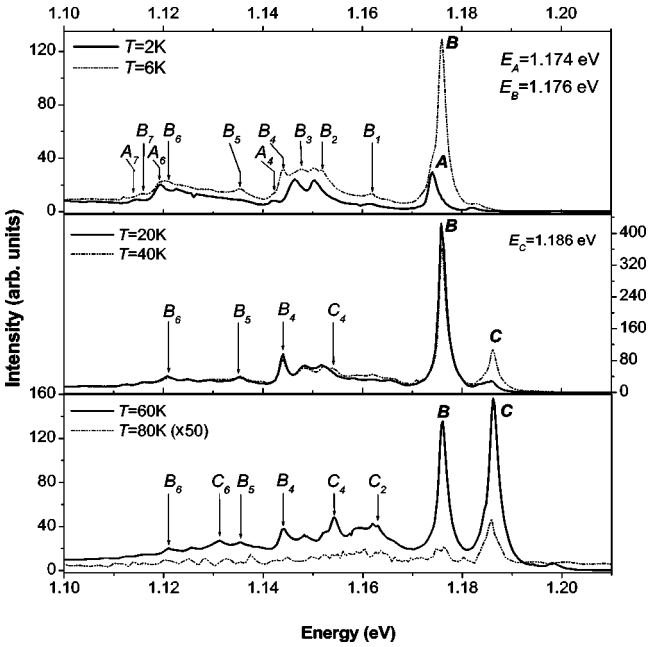

FIG. 2. Temperature evolution of the excitonic spectral region. At least three zero-phonon lines contribute to the radiative process. The redistribution of the PL intensity is played out through the three major lines *A*, *B*, and *C*. Several *A*, *B*, and *C* phonon replicas are shown at different temperatures (once again refer to Table I for the phonon energies).

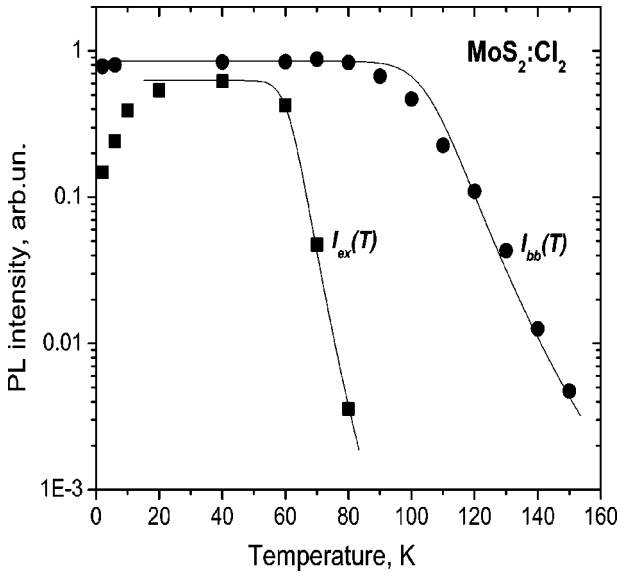

FIG. 3. Temperature dependence of the integrated intensity for the excitonic emission (■) and the broad band emission (●). The solid lines illustrate the fit of Eq. (1) to the thermal quenching behavior.

Apart from the thermal increase of the excitonic intensity at low temperatures ($T<20$ K, see the discussion below), the behavior of the $I_{ex}(T)$ and $I_{BB}(T)$ dependencies can be described by the Mott-Seitz formula

$$I_{ex,BB}(T)=C[1+C_q\exp(-E_q/kT)]^{-1} \quad (1)$$

with the activation energy $E_{q\mathrm{ex}}=0.12$ eV for the excitonic quenching and $E_{q\mathrm{BB}}=0.17$ eV for the broad band emission quenching.

III. DISCUSSION

A. Excitonic region

As was the case for the tungsten dichalcogenides,[10] the spectral distribution and temperature dependence of the sharp spectral lines of synthetic 2H-MoS_2 are very similar in behavior to the excitonic multiplets caused by the electron-hole *j-j* coupling well-known for silicon, some III-V materials and II-VI semiconductors with isoelectronic impurities.[15–17] In contrast to isoelectronically doped GaP or Si, where in the absence of external perturbations[18–21] the *j-j* coupling is manifested as a so-called *A-B* spectral doublet, the excitonic spectra of the layered MoS_2, due to the lower symmetry, involve *at least* three zero-phonon lines. It can be seen in Fig. 2 that the *B* and *C* spectral components have substructures consisting of smaller lines. The luminescent properties of the MoS_2 crystals can be attributed to the radiative recombination of excitons bound to the neutral centers, which exhibit in 2H-TX_2 layered compounds the same properties as the isoelectronic traps formed by nitrogen in GaP, resulting in efficient luminescence in an indirect band gap semiconductor. These centers in MoS_2 are formed by the halogen molecules (Cl_2 in the present case) positioned within the van der Waals gap.[10] The intercalation of the Cl_2 molecules during the crystal growth process in the well-defined sites of the MoS_2 lattice is the result of the close correspondence of the intra-molecular Cl-Cl distance ($d_{\text{Cl-Cl}}=1.98$ Å) and the characteristic dimensions of these sites. Indeed, as in other hexagonal TX_2 crystals, there are two adjacent tetrahedral coordinated interstitial sites in the MoS_2 van der Waals gap (see Fig. 4) of which the distance between the centers ($d_{\mathrm{int}}=2.13$ Å) is close to the $d_{\text{Cl-Cl}}$ value. The transverse diameter of the Cl_2 molecules is also well matched to the interstitial sites' sizes; this diameter is also smaller than the thickness of the van der Waals gap ($h\approx 3$ Å), thereby making possible an effective intercalation of the gaseous transport agent into the layered crystal during its growth. Because of their large electronic affinity, the neutral halogen molecules arranged between the *X-T-X* sheets can exhibit properties of electron-attractive centers,[22] creating a short-range potential similar to that of the isoelectronic traps in GaP. The conclusion that the radiative centers in synthetic 2H-MoS_2 single crystals are formed by the transport agent halogen molecules is supported by the absence of the excitonic luminescence in the natural (without halogen) MoS_2 samples. It should be noted that the effects of halogens (bromine) on the low-temperature conduction processes in $MoTe_2$ layered crystals were unambiguously demonstrated in Ref. 23.

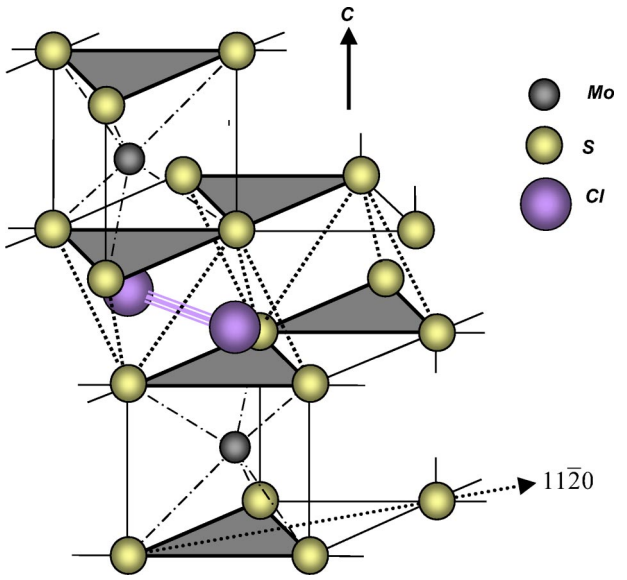

FIG. 4. Structural arrangement for 2H-MoS_2 with a diatomic halogen molecule in the van der Waals gap.

The increase with temperature of the short-wavelength emissions integral intensity at $T<20$ K, as well as the redistribution of the PL intensity between the *A*, *B*, and *C* lines can be explained with the well known temperature behavior of the bound excitons radiative lifetime $\tau_R(T)$.[16,19]

In thermal equilibrium conditions at the lowest temperatures the τ_R value is determined by the lifetime τ_A of the excitonic state *A* (responsible for the *A* line). Since the transitions from this state are dipole forbidden,[16,19] the τ_A value is much higher than the lifetime τ_B and still higher than τ_C, corresponding to the allowed radiative transitions from *B* and *C* states respectively ($\tau_A \gg \tau_B > \tau_C$). The thermal population of the *B* state ($E_B-E_A=\delta_{BA}\approx 2$ meV) leads to an increase of the radiative recombination rate $\tau_R^{-1}(T)$ starting from τ_A^{-1} at $T=2$ K up to τ_B^{-1} at $T\approx 20$ K and to the reduction and formation of the *A* and *B* line, respectively, in the steady-state spectra in Fig. 2 (because of the inequality $\delta_{BA}\ll\delta_{CB}=E_C-E_B=10$ meV, the influence of the *C* state can be neglected in this temperature range). It can be shown that if there is a channel for nonradiative excitonic recombination with a lifetime commensurable to the τ_R value, then a dramatic shortening of the lifetime $\tau_R(T)$ may be responsible for the increase of the radiative recombination efficiency observed in the 2 to 20 K range. Further temperature increases lead to the population of the upper *C* state (with the shortest radiative lifetime) and to the appearance of the *C* spectral line. The lifetimes could not be experimentally determined due to the slow response of the cooled Ge detector.

B. Broad-band region

The spectral shape of the broad band observed for both types of MoS_2 samples, and the relationship between the energy values $E_g^{\mathrm{ind}}-E_{\mathrm{BB}}=0.34$ eV and $E_{q\mathrm{BB}}=0.17$ eV sug-

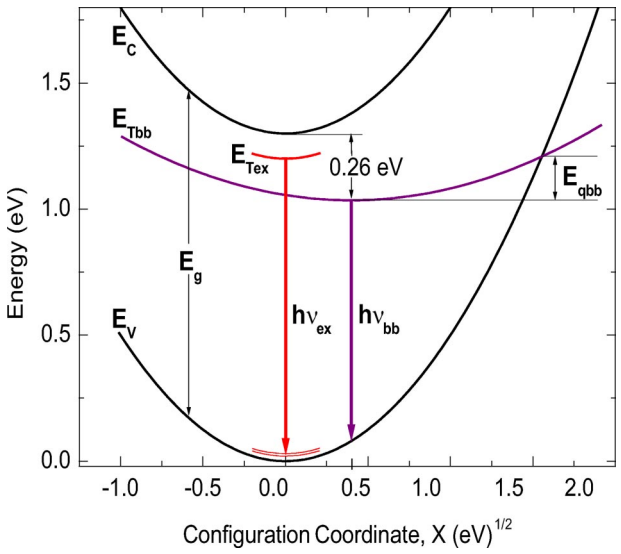

FIG. 5. Single configuration coordinate diagram illustrating the recombination processes in 2H-MoS_2:Cl_2 layered crystals. E_C, E_V, and E_{TBB} represent the conduction band, the valence band and the deep level responsible for the broad band luminescence ($h\nu_{BB}$: transition). The thermal quenching of the broad band, with activation energy E_{qBB}, takes place via the crossing point of the E_V and E_{TBB} parabolas. E_{Tex} represents the potential-well energy of the electron-attractive center induced by the halogen molecule ($h\nu_{ex}$: excitonic radiative transition).

gest that this emission occurs as a result of radiative transitions between a deep donor center and the valence band in the conditions of a strong electron-phonon coupling.[20,24,25] The two steps on the high-energy wing of the band at $E_{BB1}=1.017$ eV and $E_{BB2}=0.996$ eV seen in Fig. 1 can be attributed to the first and second phonon replicas of the zero-phonon radiative transition. The distance between them corresponds to the energy of the local vibronic mode, $E_{ph5}\approx 22$ meV, involved in the phonon coupling to the optical transition. Thus, the electronic zero-phonon transition value of $E_{BB0}=1.04$ eV for the broad band can be obtained.

The single configuration coordinate diagram (CCD) of the deep center T_{BB} with potential energy E_{TBB} responsible for broad-band emission in the 2H-MoS_2 crystal was constructed (Fig. 5). The energy values E_{BB}, E_{qBB}, Δ_{BB}, E_g^{ind} were used and the phonons energies E_{LO} and E_{ph5} (the local mode) were assumed to correspond to the vibrational quanta of the carrier in the free (ground) and trapped (excited) states, in the frame of the semiclassical approximation.[26] The E_{Tex} zero offset potential associated with the excitonic luminescence was drawn taking into account the fact that $E_{qex}\cong 0.12$ eV, as well as considering the weakness of the electron-phonon coupling inherent in isoelectronic centers [typical value of the Huang-Rhys factor $S=0.2$–0.3 (Refs. 27,28)]. It should be noted that a donor level located at about 0.25 eV below the conduction band was also observed from electrical transport data.[23,29] According to Ref. 29, this level can be attributed to a native defect of the MoS_2 crystal, but the species were unidentified.

The intensity of the broadband emission does not depend on the excitonic recombination efficiency—the quenching of the band takes place only when the sharp lines have totally vanished. This indicates that the recombination rate via the broadband channel is much higher than that via the excitonic one. Therefore, the radiative recombination caused by the deep level can be treated as a shunt channel for the excitonic luminescence. Because of this shunt the excitonic exponential quenching should occur at temperatures when the thermal ejection rate of the electrons from the T_{ex} trap becomes more important than the rate of the excitonic radiative transitions. Detailed analysis of the recombination kinetic model for 2H-MoS_2:Cl_2, taking into consideration the competition between the two channels will be given in a forthcoming paper.

IV. CONCLUSION

Halogen molecules, used as transport agents in single crystal growth, can intercalate between the layers of molybdenite and can induce strong excitonic photoluminescence. This phenomenon is not restricted to 2H-MoS_2 but has also been observed in WS_2 and WSe_2 and should likely be observed in other TX_2 compounds, leading to a new class of near-infrared emitters. Attempts to intercalate halogen molecules into natural molybdenite (a relatively abundant material) have already started in the hopes of inducing the same excitonic luminescence as in the synthetic material.

ACKNOWLEDGMENTS

We would like to extend our appreciation and our most sincere thanks to R. Leonelli from the Départment de Physique de l'Université de Montréal, Canada and F. Lévy at the Laboratoire de Physique appliquée EPF in Lausanne, Switzerland for providing us with the synthetic MoS_2 samples. We gratefully acknowledge E. Bucher from the Department of Physics of Konstanz University, Germany for stimulating discussions and friendly support as well as O. Schenker for assistance with the measurements.

[1] A. Wilson and A.D. Yoffe, Adv. Phys. **18**, 193 (1969).
[2] W.J. Schutte, J.L. de Boer, and F. Jellinek, J. Solid State Chem. **70**, 207 (1987).
[3] G. Kline, K.K. Kam, R. Ziegler, and B.A. Parkinson, Sol. Energy Mater. **6**, 337 (1982).
[4] *Photoelectrochemistry and Photovoltaics of Layered Semiconductors*, edited by A. Aruchamy (Kluwer Academic Publishers, Dordrecht, 1992).
[5] R. Tenne, L. Margulis, M. Genut, and G. Hodes, Nature (London) **360**, 444 (1992).
[6] G. Seifert, H. Terrones, G. Jungnickel, and T. Frauenheim, Phys. Rev. Lett. **85**, 146 (2000).

[7] G.L. Frey, S. Elani, M. Homoyonfer, Y. Feldman, and R. Tenne, Phys. Rev. B **57**, 6666 (1998).
[8] T. Böker, R. Severin, A. Müller, C. Janowitz, R. Manzke, D. Vob, and P. Krüger, Phys. Rev. B **64**, 235305 (2001).
[9] A. Klein, S. Tiefenbacher, V. Eyert, C. Pettenkofer, and W. Jaegermann, Phys. Rev. B **64**, 205416 (2001).
[10] L. Kulyuk, E. Bucher, L. Charron, E. Fortin, A. Nateprov, and O. Schenker, Nonlinear Opt. **29**, 501 (2002).
[11] E. Fortin and W.M. Sears, J. Phys. Chem. Solids **43**, 881 (1982).
[12] S. Uchida and S. Tanaka, J. Phys. Soc. Jpn. **45**, 153 (1978).
[13] T.J. Wieting and J.L. Verble, Phys. Rev. B **3**, 4286 (1970).
[14] A.M. Stacy and D.T. Hodul, J. Phys. Chem. Solids **46**, 405 (1985).
[15] W. Czaja, Festkoerperprobleme **11**, 65 (1971).
[16] P.J. Dean and D.C. Herbert, *Excitons* (Springer, New York, 1979), Vol. 14.
[17] X. Zhang, K. Dou, Q. Hong, and M. Balkanski, Phys. Rev. B **41**, 1376 (1990).
[18] L. Merz, R.A. Faulkner, and P.J. Dean, Phys. Rev. **188**, 1228 (1969).
[19] J. Weber, W. Schmid, and R. Sauer, Phys. Rev. B **21**, 2401 (1980).
[20] M. Godlewski, W.M. Chen, M.E. Pistol, B. Monemar, and H.P. Gislason, Phys. Rev. B **32**, 6650 (1985).
[21] B. Gil, M. Baj, J. Camassel, H. Mathieu, C.B. la Guillaume, N. Mestres, and J. Pascual, Phys. Rev. B **29**, 3398 (1984).
[22] W. Jaegermann, Ber. Bunsenges. Phys. Chem. **92**, 537 (1988).
[23] S.W.H. El-Mahalawy and B.L. Evans, Phys. Status Solidi B **79**, 713 (1977).
[24] C.H. Henry and D.V. Lang, Phys. Rev. B **15**, 989 (1977).
[25] D.V. Lang, in *Deep Centers in Semiconductors: A State of the Art Approach*, edited by S.T. Panteleides (Gordon and Breach, New York, 1992).
[26] D. Curie, in *Optical Properties of Ions in Solids*, edited by B. di Bartolo (Plenum Press, New York, 1975).
[27] H. Dai, M.A. Gundersen, C.W. Myles, and P.G. Snyder, Phys. Rev. B **37**, 1205 (1988).
[28] Y. Zhang, W. Ge, M.D. Sturge, J. Zheng, and B. Wu, Phys. Rev. B **47**, 6330 (1993).
[29] A.J. Grant, T.M. Griffith, G.D. Pitt, and A.D. Yoffe, J. Phys. C **8**, L17 (1975).